Proc. Natl. Acad. Sci. USA
Vol. 91, pp. 12467–12471, December 1994
Neurobiology

Visual motion induces synchronous oscillations in turtle visual cortex

(attention/brain evolution/cortical synchrony/event-related potential/gamma rhythm)

JAMES C. PRECHTL

Neurobiology Unit, Scripps Institution of Oceanography, and Department of Neurosciences, School of Medicine, University of California, San Diego, La Jolla, CA 92093–0201

Communicated by Theodore H. Bullock, September 6, 1994

ABSTRACT **In mammalian brains, multielectrode recordings during sensory stimulation have revealed oscillations in different cortical areas that are transiently synchronous. These synchronizations have been hypothesized to support integration of sensory information or represent the operation of attentional mechanisms, but their stimulus requirements and prevalence are still unclear. Here I report an analogous synchronization in a reptilian cortex induced by moving visual stimuli. The synchronization, as measured by the coherence function, applies to spindle-like 20-Hz oscillations recorded with multiple electrodes implanted in the dorsal cortex and the dorsal ventricular ridge of the pond turtle. Additionally, widespread increases in coherence are observed in the 1- to 2-Hz band, and widespread decreases in coherence are seen in the 10- and 30- to 45-Hz bands. The 20-Hz oscillations induced by the moving bar or more natural stimuli are nonstationary and can be sustained for seconds. Early reptile studies may have interpreted similar spindles as electroencephalogram correlates of arousal; however, the absence of these spindles during arousing stimuli in the dark suggests a more specific role in visual processing. Thus, visually induced synchronous oscillations are not unique to the mammalian cortex but also occur in the visual area of the primitive three-layered cortex of reptiles.**

Synchrony has long been considered to be an important mechanism by which neurons combine information from converging sources (1). In mammals visual motion induces gamma-band oscillations (≈30–50 Hz) in primary visual cortex, and, if the motion is congruent in two places, it induces synchronization between spatially separate cortical areas (2, 3). These gamma-band oscillations have been implicated in sensory processing, including perceptual feature binding (2–6) and attention (7, 8). The oscillations have been studied mostly in the anesthetized cat but more recently also in awake, behaving monkeys (9, 10). The present finding of visually induced synchronizing oscillations in a band (15–25 Hz) that might be equivalent, adjusting for body temperature, in a reptilian cortex suggests that synchrony may be a fundamental feature of visual processing in amniotes.

In previous studies on turtles we used sequences of diffuse light flashes that included "oddball" (11) or missing stimuli (12) to study brain potentials related to apparent "surprise" or "expectation." Such stimuli evoked time-locked potentials at different levels of the visual system, and at some sites included oscillations in the 15- to 25-Hz range. In other experiments we observed similar oscillations during spontaneous vision with and without moving stimuli, often in association with shifts in gaze (13). In the present experiments we used uniform stimuli and multielectrode coherence analyses to characterize further these oscillations, their distribution, and phase relationships.

The publication costs of this article were defrayed in part by page charge payment. This article must therefore be hereby marked "*advertisement*" in accordance with 18 U.S.C. §1734 solely to indicate this fact.

MATERIALS AND METHODS

Subjects. Eight pond turtles (*Pseudemys scripta*) of both sexes were used, having carapace lengths between 16 and 17 cm. The turtles were maintained in aquaria (20–25°C) on a 14:10 hr light/dark cycle. Use and handling of the animals were under the guidelines established by the University of California, San Diego and the National Institutes of Health.

Surgery. Cold anesthesia by continuous immersion in a crushed ice slush was used (core temperature <4°C). In addition, 20% (wt/vol) benzocaine (topical) and 2% (wt/vol) lidocaine (subcutaneous) were used as local anesthetics. Head position was fixed by an aluminum frame with a bite bar to which the beak and frontal bones were anchored by screws and acrylic cement. After the dura and arachnoid membranes were partially removed, the animal was allowed to warm to room temperature (≈23°C), and a micromanipulator was used to insert the electrode array. The wound edges were painted with 5% (wt/vol) lidocaine ointment, and no signs of discomfort were evident in limb movements or the electrocardiogram.

Recording and Data Analyses. A bilateral array (Fig. 1) of 10 stainless steel semi-microelectrodes (F. Haer, Brunswick, ME; <2.0 MΩ after platinum blacking) was used. On each cerebral hemisphere four electrodes were targeted for the visual area, three of them to record from the dorsal cortex (DC) 100–200 μm below the pial surface and one of them 800 μm longer to reach the anterior part of the dorsal ventricular ridge (DVR, the terminal zone of the tecto–thalamo–telencephalic visual pathway found in birds and reptiles). A fifth more caudal electrode was 3.3 mm longer to record from the central amygdala area of the basal part of the DVR (Fig. 1). Brain recordings were monopolar with the reference electrode in the frontal sinus area. The electrooculogram was recorded with electrodes on inferior and temporal sides of the eye. Electrode placements in the brain were localized by anodal lesions and the Prussian blue reaction on 30-μm sections stained with neutral red.

Amplified potentials were band-passed between 0.1 and 50 Hz, digitized (12 bits) at 200 points per s with DataWave software (Broomfield, CO). Programs developed by M. C. McClune (BrainWave Tools, University of California, San Diego) were used for off-line analyses. Coherence was estimated and corrected for sampling bias according to the algorithm of Carter *et al.* (14). Coherence values were based on the first 10 trials without movement artifact for each animal; <30% of the trials were rejected. The poststimulus sample was the first second of the induced oscillation that began 400 ms after the start of the stimulus movement, and it was compared with 1 s of the immediately preceding prestimulus period. Coherence changes for the subject group (n = six animals) were statistically evaluated with paired, two-tailed t tests. Coherence changes for specific electrode

Abbreviations: DC, dorsal cortex; DVR, dorsal ventricular ridge.

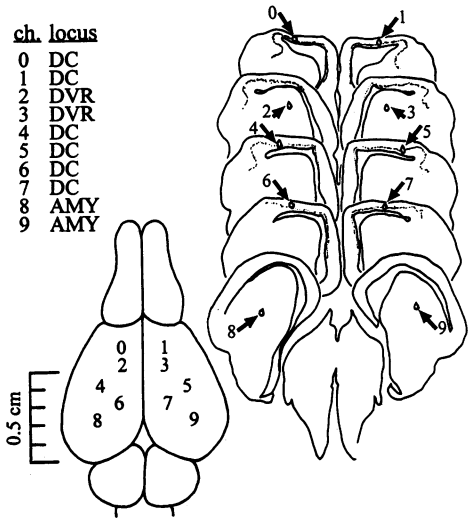

FIG. 1. (*Left*) Electrode-array configuration and list of target loci [DC, DVR, and amygdala (AMY)]. (*Right*) Sample of histologically verified loci.

placements in individuals were judged to be reproducible if successive averages (five trials each) of the coherence changes were consistently >0.1. Analyses in 10 bands between 1 and 45 Hz were averages of the coherences over a 5-Hz range and designated by a center frequency (e.g., "5" Hz = 3–7 Hz inclusive; "15" Hz = 13–17 Hz inclusive), although the "1"-Hz designator refers to <1–2 Hz.

Stimuli and Protocol. The array was lowered in 50-μm steps until 20-Hz spindles were clearly observable on one or more channels in response to moving stimuli. Trials with moving-bar stimuli began while the turtle was in a quiet, alert state, as indicated by the eyes being open, the limb movements few, and the heart rate low (<20 beats per min). Eye position or gaze was not controlled. The moving stimulus was a 3.5 × 19.5 cm black, vertical bar on a white computer screen centered 20 cm from the animal. The bar moved horizontally 3.9 cm/s and lasted 7 s before moving off the computer screen; it was restarted 5 s later. This sequence was repeated 15–30 times without interruption; in four of the animals this was followed by trials with the bar passing in the opposite direction and then again by more trials in the initial direction.

RESULTS

Time-Locked Components. Average evoked potentials to the moving bar were found in all channels, some with and some without oscillations. Those obtained in the forebrain visual areas (DC and DVR) with moving-bar stimuli are similar to flash-evoked potentials but with slower and longer latency components. The first wave after the appearance of the moving bar begins at ≈150 ms and peaks between 300 and 400 ms. Recorded above the pyramidal cell layer of the DC it has a negative polarity (N300–400) and is followed by a slower positive wave, P750–1050. Deeper DC electrode sites and those in the DVR give similar wave sequences that are opposite in polarity. Evoked potentials from amygdala electrodes, however, appear different; their waves are sharper and have shorter latencies (onset <150 ms, peak <300 ms).

Oscillations. The moving-bar stimulus evokes ≈20-Hz oscillations in the DC and DVR during several seconds with peak-to-peak amplitudes as great as 300 μV. The oscillation has a dominant frequency in the 15- to 25-Hz range and a broad band appearance in spectra based on group averages (e.g., Fig. 4*A*); however, the frequency distributions of individual responses are narrow. Moreover, measurements of successive cycles of the first 1.5 s of the oscillation from each of the six turtles yielded SEMs ranging from ±1.8 to ±3.5 ms (i.e., 0.8–1.8 Hz).

After digitally band-passing the data between 17 and 23 Hz the oscillations in a single trial appear as clusters of spindles (upper trace in Fig. 2; also Fig. 3). An early spindle group begins at 195 ± 34 ms, (mean and SEM, n = six animals), ≈50 ms after the onset of the slow potential and lasts for 2145 ± 200 ms. (Spindle onset was judged by eye as >10% increase in peak-to-peak amplitude as compared with the prestimulus average.) The spindles that compose this early group are 270 ± 17 ms in duration. These are followed by a more irregular clustering of smaller amplitude spindles. Large, late spindles (>2 s poststimulus) were observed on some trials with eye movements, as indicated by deflections in the electrooculogram. Eye movements were rare during the first seconds of spindling induced by the moving bar. Although the oscillations recorded at DC and DVR loci appear similar, the responses recorded in the amygdala are distinct in form and duration. The amygdala responses consist of sharp waves that increase in density during the stimulus but because of their irregular cycle lengths do not have the appearance of an oscillation (data not shown).

In each of six turtles tested with the moving bar 2–5 of the 10 electrodes showed 20-Hz oscillations that were reflected in significant increases in 20-Hz (i.e., 17–23 Hz) power. The frequency of the oscillation waves based on serial measurements of cycle length corresponded to the frequency peak of the power spectrum within 2–3 Hz. Accordingly, power in the 20-Hz band was used as an index of oscillation amplitude for quantitative comparisons.

Unlike the slow potential observed on all electrodes, oscillations were recorded only from visual-area electrodes. The local origin of the DC oscillations is indicated by their phase reversal at deeper placements in or below the pyramidal cell layer. In three turtles the oscillations were confined to the right hemisphere. The failure to observe left-sided oscillations in these animals may be due to the fixed configuration of the array without freedom to control the insertion of individual electrodes. Slight asymmetries in the array and differences in the ease of insertion might have caused slight dimpling and pressure on the left hemisphere. Cortical oscillations appear particularly vulnerable to pressure or trauma (15), and more recent experiments (13) with atraumatic epipial electrodes have yielded oscillations that are lower in amplitude but bilaterally robust in every turtle studied.

The amplitude and duration of the 20-Hz responses show a decline during successive trials, the average 20-Hz power of the second 10 trials was 27 ± 6% less than that of the first 10 trials. Moreover, the oscillatory responses are labile, and even in some early trials they may be indistinguishable or exceptionally small. The phase of the oscillation is not

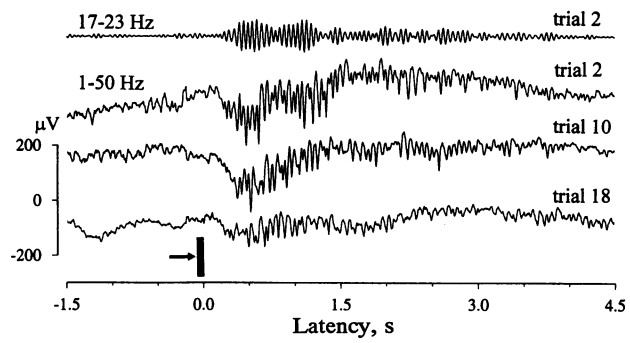

FIG. 2. Sample responses to moving bar recorded in the DC over a 3.6-min period. Bar movement begins at time zero and completes a left-to-right movement in 7 s (≈11°/s), which is followed by a 5-s rest interval. The top trace is filtered to show the 17- to 23-Hz component without any slow potential.

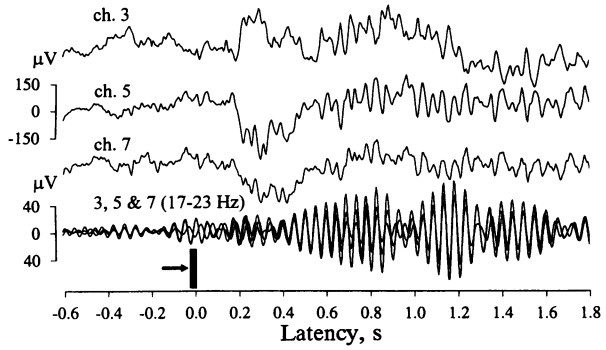

FIG. 3. Upper traces are single responses recorded from DVR [channel (ch.) 3] and DC electrodes (channels 5 and 7) before and during the moving-bar stimulus. All three electrodes show the slow potential and 20-Hz oscillations, although the DVR trace (channel 3) is opposite in phase. The same traces are superimposed on the bottom after filtering (17–23 Hz) and inverting the phase (i.e., sign reversal) of the DVR trace. Note the spindle structure and the associated phase correlation induced by the stimulus.

time-locked to the onset of the stimulus, the averaging of successive trials produces a smaller amplitude oscillation than those of the individual epochs (see also ref. 12), although the phase of the spindle envelope is time-locked within ±100 ms or so, enough to appear in averages.

Analyses of Power. In addition to identifiable oscillations, the moving-bar stimulus also evokes power increases in all bands (1–45 Hz) during the first 2–3 s. The power increases are largest in the 20-Hz band, as much as 432 ± 80% in the best loci. Power in most bands returns to control levels by the third second of bar movement; however, the 20-Hz activity does not reach control levels until the sixth or seventh second. Amygdala loci show the greatest resting power (i.e., unstimulated), particularly in frequencies <20 Hz, and some amygdala placements were distinguished by relatively large increases in power in the 40- to 45-Hz band during the stimulus. Fig. 4*A* shows the average increased power for the

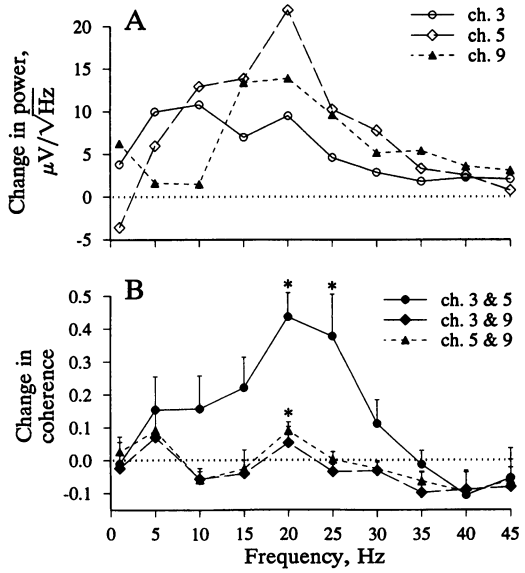

FIG. 4. (*A*) Average increases (n = six animals) in power during the first second of the oscillation for right-side visual-area channels 3 and 5 and amygdala channel (ch.) 9. (*B*) Changes in coherence between the electrodes of *A*. Note that despite the sizable increases in 20-Hz power recorded at the amygdala locus (channel 9, *A*) the coherence increase is mostly between the visual-area electrodes, channel 3 and channel 5. (Bars represent SEMs, and asterisks indicate $P < 0.05$, $n = 6$.)

group (n = six animals) recorded at three electrode sites for the first second of the response.

Coherence. The question was addressed: how congruent is the activity in different loci, in different frequency bands, before and after stimulation by visual motion? Coherence was chosen over correlational methods because it gives a value for each frequency and is normalized for the amplitude at each electrode (see Table 1).

The moving-bar stimulus induced a marked increase in coherence during the first second of the oscillation in the 15-, 20-, and 25-Hz bands between loci in the visual areas of the same hemisphere in all six animals tested (Fig. 5). In Fig. 5 each connecting line between a pair of electrodes represents a reproducible change in a single animal based on consistent coherence averages from successive groups of trials. The distribution of coherence changes is complex, but a general pattern emerges in which the increases in low and middle frequencies (1–5 and 15–25 Hz) are accompanied by decreases in the higher frequency range (30–45 Hz) and in the 10-Hz band. The increased coherences in the 20-Hz band were distinguished by their magnitude and local distribution.

Fig. 4*B* shows changes in coherence based on group averages for pairs of electrodes for which the power spectrum is given in Fig. 4*A*. Asterisks indicate statistically significant increases ($P < 0.05$, n = six animals). Although all three electrodes show substantial increases in 20-Hz power (Fig. 4*A*) the coherence increases are mostly between the visual-area electrodes (channel 3 and channel 5). Increases in 20-Hz coherence in the left hemisphere were confined to the three animals with left-side electrode placements that showed 20-Hz oscillations. Other significant changes in coherence for pooled data are given in Table 1.

The electrode pairs that showed the largest increases in 20-Hz coherence were the DC–DVR pairs (channel 3 and channel 5), for which oscillations were 180° out of phase. Fig. 3 gives an example of responses of that electrode pair and of a more caudal DC electrode (channel 7). To focus on the 20-Hz synchronization that occurs in a single trial, the three channels are filtered and superimposed at the bottom of the plot, with the phase of channel 3 inverted. Note that until ≈0.4 s after the stimulus onset the phase relations between the three channels wander; then during the oscillation they become tightly correlated for hundreds of milliseconds. Such plots affirm that the observed synchronizations are not simply the results of a common volume-conducted potential. Unlike volume-conducted signals the 20-Hz waves recorded at the different loci show dynamic phase differences as well as uncorrelated changes in amplitude. Moreover, the closest spaced cortical electrode pair (channel 1 and channel 3, Fig. 1), which would be most susceptible to volume-conduction effects, showed smaller and less reliable increases in coherence. In contrast to the focal changes in coherence in the 20-Hz band, coherence increases in the lower frequencies related to the slow potential are widespread between ipsilateral, cortical, amygdalar, and interhemispheric loci (Fig. 5,

Table 1. Pairs of recording loci with significant changes in coherence

Recording loci pairs								
1 Hz	5 Hz	10 Hz	15 Hz	20 Hz	25 Hz	30 Hz	35 Hz	40 Hz	45 Hz
	+3,7	+3,7	+3,7	+3,5	+3,5	+0,6		−2,4	−4,7
			+5,7	+3,7		+1,7		−6,8	
				+5,9		−2,4			
						−4,7			

Pairs of recording electrodes (loci shown in Fig. 1) and frequencies with significant increases (+) or decreases (−) in coherence in the first second of the induced oscillation ($P < 0.05$, $n = 6$).

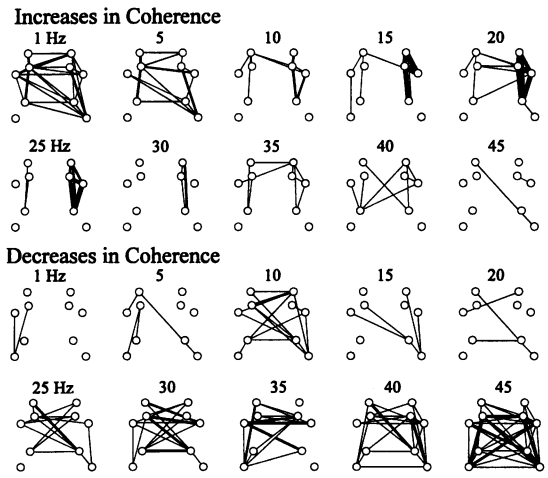

FIG. 5. Maps of coherence changes during visual motion combined from six animals based on electrode configuration as shown in Fig. 1. Each connecting line represents an electrode pair in a single animal for which coherence was found to consistently change by >0.1 in two independent estimates (five trials each) based on 1-s samples (prestimulus and poststimulus).

1–10 Hz). The coherence decreases in the higher frequencies (30–45 Hz) have a similarly broad distribution (Fig. 5 *Lower*).

Effects of Arousal and Illumination. The moving-bar stimulus may also have arousing effects. In reptiles increased electroencephalogram power in the higher frequencies (>12 Hz) has been attributed to arousal (16, 17). To separate possible arousal effects from those related to vision the responses to visual stimulation (experimenter hand movements) were compared with responses to brief tail pinches given in complete darkness. The pinches elicit hind limb scratching movements, large increases in heart rate (>200%), and broad band increases in electroencephalogram power, greatest between 1 and 14 Hz (Fig. 6). The visual stimuli also

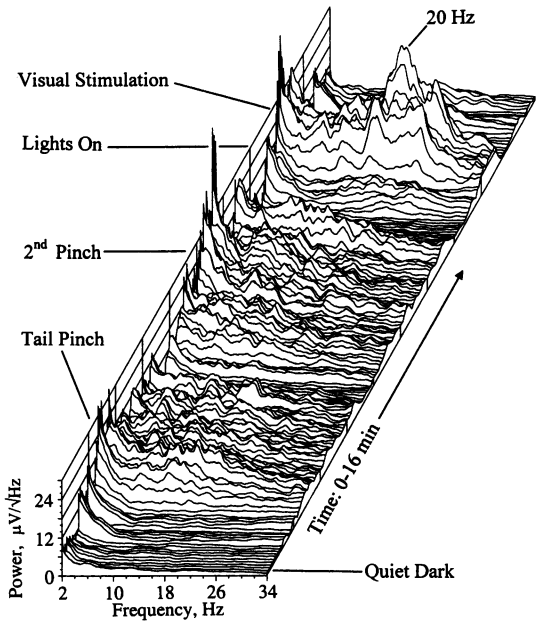

FIG. 6. Moving average of successive power spectra during behavioral states after quiet rest in the dark, brief tail pinches, and moving visual stimuli. Tail pinches cause broad increases in power of the cortical electroencephalogram and increases in heart rate. After the lighting is returned, visual stimulation (experimenter hand movement) is also arousing, as measured by heart rate increases, but in addition it uniquely elicits prominent peaks of power in the 20-Hz band.

increase heart rate and broad band cortical activity, but with a distinctive peak in the 20-Hz region of the cortical power spectrum (Fig. 6) related to 15- to 25-Hz oscillations in the local field potential.

The 15- to 25-Hz spindles and associated slow potentials also occur spontaneously in visual area electrode records without moving visual stimuli and in association with shifts in gaze. When 5 min of spontaneous records under standard room illumination was compared with an immediately following 5-min period in darkness, the power spectra under the illuminated condition show between 100 and 150% more power in the 15- to 20-Hz band, without any comparable increase in other bands.

DISCUSSION

The main finding is that visual motion induces spindle-like bursts of 20-Hz oscillations (i.e., 15–25 Hz) in the local-field potentials of the visual cortex. During the oscillations increases in 20-Hz synchrony, as measured by coherence analysis, occur to differing extents between some of the ipsilateral loci. The response begins with a surface-negative slow potential (1–5 Hz), which is coherent between widespread bilateral visual and nonvisual areas. At the same time widespread decreases in coherence occur in the 10- and 35- to 45-Hz bands. The oscillations appear to be induced specifically by visual aspects of the stimulus because equally arousing cutaneous or auditory stimuli presented in the dark will not trigger them. Similar appearing spindles are also observed in the absence of moving or changing visual elements but in association with visual behaviors such as shifts of gaze.

Analyses of superimposed sweeps from different electrodes indicate that the coherence increases between visual loci are due to the increased phase correlation of 20-Hz waves during the oscillation. Although the dominant frequency of the oscillation ranges from 15 to 25 Hz and has a broad band appearance in spectra based on group averages (e.g., Fig. 4*A*), the cycle lengths in individual responses are sufficiently regular to appear oscillatory. Amygdala responses, however, do not include 20-Hz oscillations, even though their spectra show large peaks in this band. Rather, increases in 20-Hz activity in the amygdala are due to large sharp waves that increase in density during the response but without showing regular 40- to 60-ms cycles. Moreover, the increases in the 20-Hz power of amygdala responses are associated with little or no increase in coherence with the other loci.

The distribution and origins of the oscillations are complicated by the contribution of volume conduction between the closely spaced electrodes. The DC is considered to be at least one origin of the oscillations because the phase of the DC oscillation and the associated slow potential reverse as an electrode is lowered from the cortical surface a few hundred micrometers to the pyramidal cell layer. When the structures of oscillations from neighboring DC electrodes are closely compared, they provide evidence of multiple origins on the basis of their variable phase differences and uncorrelated amplitude modulations. Passive spread from a single source would also fail to account for the differential patterns of coherence decreases and increases and the synchronization of responses that are opposite in phase. Moreover, the coherence does not correlate with interelectrode distance; for example, electrodes 1 and 3 were much closer than 1 and 7 but consistently showed less coherence, either resting or stimulated.

Electrodes were placed in the DVR because it is the primary projection zone of the tecto–thalamo–telencephalic pathway visual pathway found in birds and reptiles. Whereas the DC pathway is similar to the geniculocortical system of mammals, the DVR system is hypothesized to be analogous to the colliculo–thalamo–extrastriate cortical pathway (18). The DC and DVR are reciprocally connected (19, 20) and

respond comparably to light flashes (12, 21). Although the 20-Hz oscillations recorded in the DVR are large in amplitude, consistent with a local origin of the potential, the depth profile of the response does not show a phase reversal. This result might be because of the nonlaminar organization of the DVR. More analyses, including observations on single-unit responses, will be needed to map the neuron populations involved in DC and DVR responses.

DC oscillations in the 15- to 25-Hz range are not uniquely elicited by moving stimuli: similar but shorter single spindles are often observed after abrupt visual stimuli such as light flashes (12, 21), step changes in luminance, and after the termination of a flash train (12). Such stimuli have also elicited oscillations of similar frequency in the optic tectum of the ray (22, 23), not yet seen in the forebrain. Although moving bars are effective in eliciting 20- to 50-Hz oscillations in the pigeon tectum (24), the necessity of movement in this case is unclear.

Until the present report, to my knowledge, stimulus-induced oscillations that synchronize across different cortical loci have been found only in mammals. The finding of induced oscillations in the turtle's primitive, three-layered cortex affirms that, as for the rabbit olfactory bulb (25), neither a columnar nor punctate topographic organization is required. Visual cortical oscillations in cat and monkey that are thought to preattentively bind features from different parts of the visual field have shown a wide range of frequencies (30–100 Hz), depending on species and experimental conditions (2–6, 9, 10). The lower frequency oscillations in the turtle's visual cortex may be consistent with the longer latency of responses in ectotherms that have low body temperatures and low metabolic rates. DC oscillations in the turtle appear to share some general features with visual-cortex gamma oscillations in mammals: (*i*) In both taxa the oscillations are not time-locked to the stimulus (26, 27) and are therefore attenuated by averaging. (*ii*) The individual spindles in both taxa last from tens to a few hundreds of milliseconds (27, 28). (*iii*) The shape and duration of the spindles are, so far, unpredictable with respect to stimulus characteristics (28). (*iv*) The coherence between oscillations is also not perfectly stationary in that not all cycles are equally synchronized, and after 5–10 cycles of synchrony oscillations may abruptly shift in phase up to 100° or more, within two or three cycles (28).

A striking feature of the turtle's response is the duration of the oscillation. It can consist of a train of spindles that lasts for seconds in parallel with significant elevations in coherence. Another feature that may be unique to the turtle's response is the concomitant decrease in synchrony seen in neighboring bands (i.e., 10 Hz and 30–45 Hz). This effect was not suggested by the appearance of spindles or by stimulus-related differences in the power spectrum. Without the use of the coherence analysis the changes in 30- to 45-Hz bands would have gone unnoticed. Coherence calculation has rarely (29) been reported in mammals.

Cortical oscillations in gamma and beta frequency ranges have also been linked to afferent processing involving attention and orienting behaviors. Attentive sniffing in a motivated rabbit elicits 55- to 75-Hz olfactory lobe oscillations (30), and a monkey's manual exploration for a raisin elicits large 25- to 35-Hz oscillations in the sensorimotor cortex (7). Similarly, attentive visual behaviors cause large increases in 15- to 25-Hz activity in the visual cortex of cat (31) and dog (32), as well as increases in the 20- to 40-Hz range in the monkey (33). The oscillations observed in the awake turtle may also represent attention-sensitive responses because they occur with spontaneous shifts of gaze (13) and they are largest in response to salient, or attention-capturing, stimuli, such as the investigator's hand movements.

The anatomical substrates of most cortical oscillations are unknown, but some appear to be based on common thalamo–cortical input (34) or cortico–thalamic loops (31), and others seem to be based on reciprocal cortico–cortical connections (6). The anatomy of the turtle's visual system allows for the same possibilities. The DC has reciprocal thalamocortical projections and extensive connections within itself by axons that run rostrally and caudally through its extent (19).

The perceptual and cognitive differences between reptiles and mammals are poorly understood, as are the underlying forebrain differences. The basic perceptual or modulatory mechanisms attributed to synchronous cortical oscillations, if valid, may have originated in an ancestral brain similar to that of the turtle. To achieve fine-grained comparisons with mammalian gamma oscillations analyses of stimulus specificity will be needed as well as observations on the receptive-field properties of the involved neurons.

I thank A. Brzozowska-Prechtl for her assistance in histological technic. The author held a National Research Service Award and a McDonnell–Pew fellowship and was aided by National Institute of Neurological Disorders and Stroke grants to T. H. Bullock.

1. Bullock, T. H. (1993) *How Do Brains Work?* (Birkhäuser, Boston).
2. Eckhorn, R., Bauer, R., Jordan, W., Brosch, M., Kruse, W., Munk, M. & Reitböck, H. J. (1988) *Biol. Cybern.* **60,** 121–130.
3. Gray, C. M. & Singer, W. (1989) *Proc. Natl. Acad. Sci. USA* **86,** 1698–1702.
4. Gray, C. M., König, P., Engel, A. K. & Singer, W. (1989) *Nature (London)* **338,** 334–337.
5. Engel, A. K., König, P., Gray, C. M. & Singer, W. (1990) *Eur. J. Neurosci.* **2,** 588–606.
6. Engel, A. K., König, P., Kreiter, A. K. & Singer, W. (1991) *Science* **252,** 1177–1179.
7. Murthy, V. N. & Fetz, E. E. (1992) *Proc. Natl. Acad. Sci. USA* **89,** 5670–5674.
8. Niebur, E., Koch, C. & Rosin, C. (1993) *Vision Res.* **33,** 2789–2803.
9. Kreiter, A. K. & Singer, W. (1992) *Eur. J. Neurosci.* **4,** 369–375.
10. Eckhorn, R., Frien, A., Bauer, R., Woelbern, T. & Kehr, H. (1993) *NeuroReport* **4,** 243–246.
11. Prechtl, J. C. & Bullock, T. H. (1993) *J. Cognit. Neurosci.* **5,** 177–187.
12. Prechtl, J. C. & Bullock, T. H. (1994) *Electroencephalogr. Clin. Neurophysiol.* **91,** 54–66.
13. Prechtl, J. C. & Bullock, T. H. (1994) *Physiologist* **37,** 72 (abstr.).
14. Carter, C., Knapp, C. H. & Nuttall, A. H. (1973) *IEEE Trans. Audio Electroacoust.* **AU-21,** 337–344.
15. Bouyer, J. J., Montaron, M. F., Vahnee, J. M., Albert, M. P. & Rougeul, A. (1987) *Neuroscience* **22,** 863–869.
16. Hunsaker, D., II, & Lansing, R. W. (1962) *J. Exp. Zool.* **149,** 21–32.
17. Huntley, A. C. (1987) *Comp. Biochem. Physiol.* **86,** 325–330.
18. Karten, H. J. & Shimizu, T. (1990) *J. Cognit. Neurosci.* **1,** 291–301.
19. Balaban, C. D. (1978) *Anat. Rec.* **190,** 330–331.
20. Desan, P. H. (1988) in *The Forebrain of Reptiles,* eds. Schwerdtfeger, W. K. & Smeets, W. J. A. J. (Karger, Basel), pp. 1–11.
21. Prechtl, J. C. & Bullock, T. H. (1992) *NeuroReport* **3,** 801–804.
22. Bullock, T. H., Hofmann, M. H., Nahm, F. K., New, J. G. & Prechtl, J. C. (1990) *J. Neurophysiol.* **64,** 903–914.
23. Bullock, T. H., Karamürsel, S. & Hofmann, M. H. (1993) *J. Comp. Physiol. A* **172,** 501–510.
24. Neuenschwander, S. & Varela, F. J. (1993) *Eur. J. Neurosci.* **5,** 870–881.
25. Freeman, W. J. (1959) *J. Neurophysiol.* **22,** 644–666.
26. Gray, C. M., Engel, A. K., König, P. & Singer, W. (1990) *Eur. J. Neurosci.* **2,** 607–619.
27. Eckhorn, R., Reitböck, H. J., Arndt, M. & Dicke, P. (1990) *Neural Comput.* **2,** 293–307.
28. Gray, C. M., Engel, A. K., König, P. & Singer, W. (1992) *Vision Neurosci.* **8,** 337–347.
29. Bressler, S. L., Coppola, R. & Nakamura, R. (1993) *Nature (London)* **366,** 153–156.
30. Freeman, W. J. & Skarda, C. A. (1985) *Brain Res. Rev.* **10,** 147–175.
31. Bekisz, M. & Wrobel, A. (1993) *Acta Neurobiol. Exp.* **53,** 175–182.
32. Lopes da Silva, F. H., van Rotterdam, A., Storm van Leeuwen, W. & Tielen, A. M. (1970) *Electroencephalogr. Clin. Neurophysiol.* **29,** 260–268.
33. Freeman, W. J. & van Dijk, B. W. (1987) *Brain Res.* **422,** 267–276.
34. Bouyer, J. J., Tilquin, C. & Rougeul, A. (1983) *Electroencephalogr. Clin. Neurophysiol.* **55,** 180–187.